

## ISTP observations of plasmoid ejection: IMP 8 and Geotail

J. A. Slavin,<sup>1</sup> D. H. Fairfield,<sup>1</sup> M. M. Kuznetsova,<sup>1</sup> C. J. Owen,<sup>2</sup> R. P. Lepping,<sup>1</sup>  
S. Taguchi,<sup>3</sup> T. Mukai,<sup>4</sup> Y. Saito,<sup>4</sup> T. Yamamoto,<sup>4</sup> S. Kokubun,<sup>5</sup>  
A. T. Y. Lui,<sup>6</sup> and G. D. Reeves<sup>7</sup>

**Abstract.** IMP 8 and Geotail observations of traveling compression regions (TCRs) and plasmoids, respectively, are used to investigate plasmoid formation and ejection. One year of IMP 8 magnetometer measurements taken during the distant tail phase of the Geotail mission were searched for TCRs, which signal the release of plasmoids down the tail. A total of 10 such intervals were identified. Examination of the Geotail measurements showed that this spacecraft was in the magnetotail for only three of the events. However, in all three cases, clear plasmoid signatures were observed at Geotail. These plasmoids were observed at distances of  $X = -170$  to  $-197 R_E$ . The in situ plasma velocities in these plasmoids are found to exceed the time-of-flight speeds between IMP 8 and Geotail suggesting that some further acceleration may have taken place following release. The inferred lengths of these plasmoids,  $\sim 27$ – $40 R_E$ , are comparable to the downtail distance of IMP 8. This indicates that TCR at IMP 8 can be caused by plasmoids forming not only earthward but also adjacent to or just tailward of the spacecraft. The closeness of IMP 8 to the point of plasmoid formation is confirmed by the small,  $\sim 0$ – $3$  min, time delays between the TCR perturbation and substorm onset. In two of the plasmoid events, high-speed earthward plasma flows and streaming energetic particles were measured in the plasma sheet boundary layer surrounding the plasmoid along with large positive  $B_z$  at the leading edge of the plasmoid suggesting that the core of the plasmoid was “snow plowing” into flux tubes recently closed at an active distant neutral line. In summary, these unique two-point measurements clearly show plasmoid ejection near substorm onset, their rapid movement to the distant tail and their further evolution as they encounter preexisting  $X$  lines in the distant tail.

### 1. Introduction

One of the most important developments during the previous decade was the observation of “plasmoids” moving down the tail during substorms in much the manner originally envisaged by Schindler [1974] and Hones [1976]. A plasmoid is a three-dimensional segment of the plasma sheet that is ejected down the magnetotail following substorm onset. Critical ISEE 3, Galileo, and Geotail observations supporting the existence of plasmoids include high-speed tailward flows in the plasma sheet [Hones et al., 1984; Baker et al., 1987; Machida et al., 1994; Frank et al., 1994; Mukai et al., 1996], magnetic field variations consistent with quasi-closed loop or quasi-flux rope topologies

[Slavin et al., 1989; Moldwin and Hughes, 1991; Lepping et al., 1995; Slavin et al., 1995; Khurana et al., 1995; Kivelson et al., 1996; A. Ieda et al., Statistical analysis of plasmoid evolution with Geotail observations, submitted to *Journal of Geophysical Research*, 1997], isotropic and unidirectional energetic electron distributions within closed loop [Scholer et al., 1984] and flux rope-type [Belehaki et al., 1996] plasmoids, respectively, energetic ion anisotropies and three-dimensional plasma flows indicating the envelopment of the spacecraft by a bulge in the plasma sheet [Richardson et al., 1987; Owen and Slavin, 1992; Kawano et al., 1994], and traveling compression regions (TCRs) in the surrounding lobes [Slavin et al., 1984, 1993; Taguchi et al., 1997]. It has also been shown that the majority of well-defined, isolated substorms produce plasmoid signatures in the deep tail [Slavin et al., 1992; Moldwin and Hughes, 1993; Nagai et al., 1994] and that most plasmoids, in turn, are observed following substorm onset signatures near the Earth [Baker et al., 1987; Moldwin and Hughes, 1992a; Slavin et al., 1993; Zong et al., 1996]. A rich literature of numerical simulations now also exists describing plasmoid formation, topology, and ejection [e.g., Bim et al., 1989; Ogino et al., 1990; Hesse and Bim, 1991; Raeder, 1994; Walker and Ogino, 1996].

Traveling compression regions are several minute long enhancements of the magnetic field intensity in the lobes of the tail which are accompanied by a north-then-south variation in the  $B_z$  component [Slavin et al., 1984]. The original interpretation that these field signatures are caused by the draping of lobe flux tubes about plasmoids moving rapidly tailward has

<sup>1</sup>Laboratory for Extraterrestrial Physics, NASA Goddard Space Flight Center, Greenbelt, Maryland.

<sup>2</sup>Astronomy Unit, Queen Mary and Westfield College, London, England, United Kingdom.

<sup>3</sup>Department of Electronic Engineering, University of Electro-Communications, Tokyo, Japan.

<sup>4</sup>Institute of Space and Astronautical Science, Sagami-hara, Kanagawa, Japan.

<sup>5</sup>Solar-Terrestrial Environment Laboratory, Nagoya University, Toyokawa, Japan.

<sup>6</sup>Applied Physics Laboratory, Johns Hopkins University, Laurel, Maryland.

<sup>7</sup>Los Alamos National Laboratory, Los Alamos, New Mexico.

been supported by subsequent observational [Murphy *et al.*, 1987; Owen and Slavin, 1992; Slavin *et al.*, 1993; Kawano *et al.*, 1994] and theoretical [Raeder, 1994] studies. This local compression of the lobe magnetic field then accompanies the plasmoid as it moves down the tail and can be observed by spacecraft residing in the lobes. In this manner the detection of a TCR can serve as a proxy for direct plasmoid encounters for studies requiring only the knowledge of plasmoid time of release and general dimensions [e.g., Slavin *et al.*, 1992].

In this study we seek to make two point observations of the same plasmoid as it moves down the tail. Lacking a spacecraft with appropriate instrumentation stationed in the cis-lunar plasma sheet, where plasmoids first form and are ejected, we will make use of IMP 8 lobe magnetic field measurements and use TCR as proxies for the plasmoids themselves at this distance. Geotail observations are then used to directly observe the plasmoid in the distant tail. The overarching purpose of this study is to extend our knowledge of how plasmoids form and are ejected down the tail and to further test and refine the near-Earth neutral line (NENL) model that forms the theoretical basis for much of our understanding of deep-tail substorm phenomenon. Specific questions to be asked include the following: (1) When a TCR is seen at IMP 8 is a plasmoid always observed later at a greater downstream distance by Geotail? (2) How do the inferred lengths of the plasmoids compare with the downstream distance of IMP 8? (3) Do the time delays between the observation of TCRs at IMP 8 and plasmoids at Geotail indicate a time-of-flight speed which are consistent with the in situ speeds measured in the plasmoid at Geotail or is some additional acceleration/deceleration required? (4) Do the tail lobes at IMP 8 distances exhibit magnetic flux loading and the plasma sheet thinning prior to plasmoid release? and (5) Does plasmoid release take place near substorm expansion onset or significantly later as suggested by the Kiruna conjecture [Kennel, 1992]? Overall these multi-spacecraft ISTP observations will be shown to confirm many of the predictions of the near-Earth neutral line model of substorms and to yield new information regarding the manner in which plasmoids form and evolve as they encounter preexisting active X lines in the more distant tail.

## 2. Approach

For the purposes of this study we have surveyed 13 months of IMP 8 magnetic field measurements, i.e., September 1993 to October 1994, to identify all TCR events during this interval. As noted earlier, studies of the ISEE 3 and Geotail measurements [e.g., Nagai *et al.*, 1994] have shown that a spacecraft stationed at or beyond about the orbit of the moon frequently observes one or more plasmoids and/or TCRs following a substorm onset. Earthward of lunar orbit the frequency with which TCRs and, by inference, plasmoids are observed decreases until at IMP 8 only ~10–15% of all substorms produce such signatures [Slavin *et al.*, 1990; Taguchi *et al.*, 1997].

Traveling compression regions in this study were identified in the IMP 8 measurements in the same manner as in previous studies [e.g., Taguchi *et al.*, 1997]. Briefly, short-duration compressions of the lobe field lasting from tens of seconds to minutes are noted and the associated variations in the vector field components are examined. A TCR is generally defined by a north-then-south tilting of the  $B_z$  component of the field with the inflection point near the time of peak lobe field compression. However, the TCR perturbations in  $B_z$  observed at IMP

8 do not usually exhibit the more sinusoidal shapes often observed farther down the tail by ISEE 3 and Geotail. First, the initial northward tilting of the field can appear truncated or nearly absent relative to the very pronounced southward tilting. Slavin *et al.* [1990] and Taguchi *et al.* [1997] suggested that this was due to IMP 8 usually being located earthward of the region where plasmoid formation is taking place and therefore not able to observe the complete draping signature. Second, Taguchi *et al.* [1997] have shown that the lobe field flaring at IMP 8 distances is sufficient to produce an "offset" in the background lobe field so that  $B_z$  never becomes positive during the TCR. In this case the north-then-south tilting is a perturbation relative to the background flared lobe field. The search of IMP 8 magnetic field records as part of this study yielded a total of 10 TCR events. Nine of the events contained a single TCR, while one exhibited two TCRs separated by ~5 min.

Many excellent examples of plasmoids in the Geotail magnetotail measurements can be found in literature [e.g., Frank *et al.*, 1994; Mukai *et al.*, 1996]. In this study, the measurements returned by the magnetic field investigation (MGF) [Kokubun *et al.*, 1994], the plasma analyzer (LEP) [Mukai *et al.*, 1994], and the energetic particle analyzer (EPIC) [Williams *et al.*, 1994] were examined for intervals surrounding each of the TCR events identified in the IMP 8 magnetic field observations. The primary defining criteria for the plasmoids, as discussed earlier, are the observation of fast, tailward flowing plasma sheet coincident with a north-then-southward rotation of the magnetic field [e.g., see A. Ieda *et al.*, submitted manuscript, 1997]. A further caveat is that if the spacecraft is located at just the proper distance from the midplane of the tail, then it can observe a so-called boundary layer plasmoid as opposed to a plasmoid proper or a TCR [Moldwin and Hughes, 1992c]. In this case the north-south magnetic field deflection characteristic of plasmoids and TCRs is still observed, but the spacecraft stays immersed in the PSBL.

The large radial distance of Geotail when it was in the distant tail results in even small variations in the solar wind flow angles causing large changes in the location of the tail in the  $Y$ - $Z$  plane [see Zwickl *et al.*, 1984; Slavin *et al.*, 1985]. Hence probability of having both IMP 8 and Geotail inside the magnetotail for an hour or more so that two point measurements of plasmoid motion could be made is not large. For this reason it was not surprising that our examination of the Geotail magnetic field and plasma measurements showed that this spacecraft was located inside the tail for only 3 of the 10 TCR identified by IMP 8. The dates of these events are April 16, 1994, April 17, 1994, and September 26, 1994. However, each interval was found to contain a plasmoid signature, confirming that the TCRs at IMP 8 were, indeed, associated with the tailward ejection of plasmoids. In the sections to follow, the IMP 8 and Geotail measurements taken during each of these three intervals will be presented along with supporting ground-based and geosynchronous substorm observations.

### 2.1. April 16, 1994, Event

The first IMP 8/Geotail event occurred on April 16, 1994. Figure 1 displays 90 min of simultaneous, 3-s-averaged magnetic field observations from IMP 8 at  $X = -29 R_E$  and Geotail at  $X = -197 R_E$ . The low variance, largely  $X$ -directed magnetic fields in the lower panels indicate that IMP 8 was located in the south lobe of the tail throughout this interval. At 2005 UT a TCR is clearly visible in the IMP 8 measurements as a brief field compression accompanied by a

sharp southward tilting in  $B_z$  and a slower recovery. The lack of a significant  $B_y$  variation suggests that the spacecraft passed directly over the plasmoid as opposed to being off to the east or west [e.g., Slavin *et al.*, 1989] or that the plasmoid extended across much of the tail [e.g., Walker and Ogino, 1996]. During the 50 min preceding the TCR the lobe field intensity at IMP 8 steadily increased by  $\sim 25\%$  in a very typical substorm growth phase [Caan *et al.*, 1975]. The TCR coincides with the broad maximum in lobe field strength which is seen to decrease afterward.

The Geotail magnetic field measurements in the top panels of Figure 1 show the spacecraft first residing in the plasma sheet, where the field is weak and variable, and then the PSBL or north lobe where the field is much stronger. The most salient feature in the Geotail measurements is the plasmoid centered on  $\sim 2032$  UT which is indicated by the large amplitude north-then-south  $B_z$  variation accompanied, in contrast with the TCR in the lower panels, by a weakening of the field strength. Note also the very typical slow recovery of the southward  $B_z$  field following the plasmoid due to the reconnection of lobe flux tubes following plasmoid ejection. The time-of-flight speed for this plasmoid from where the TCR was observed at IMP 8 to Geotail is  $168 R_E/27 \text{ min} \sim 664 \text{ km/s}$ .

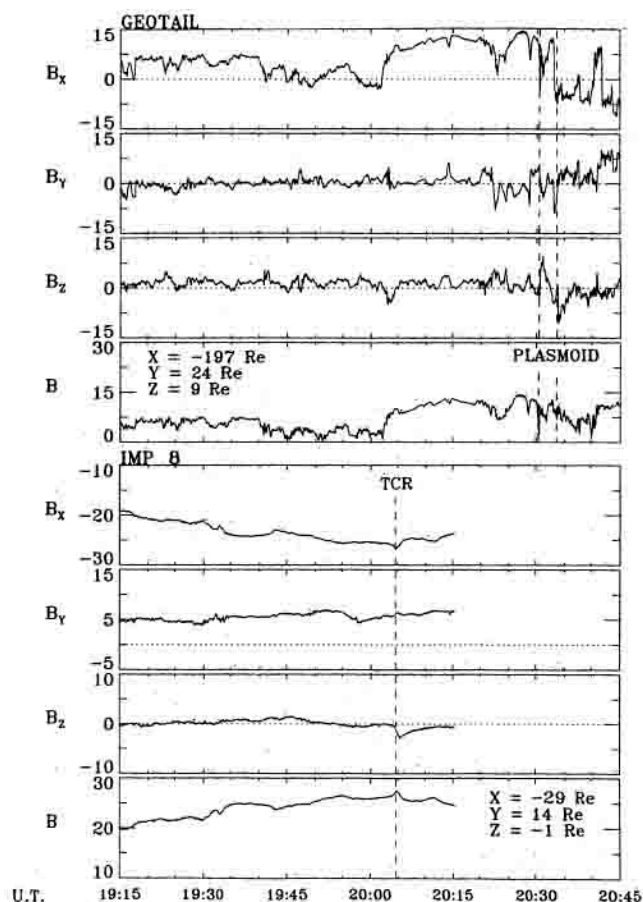


**Figure 1.** Simultaneous 3-s-averaged magnetic field measurements taken by Geotail and IMP 8 from 1915 to 2045 UT on April 16, 1994, are displayed in GSM coordinates. For this event the plasmoid at Geotail follows by 27 min the observation of the TCR at IMP 8. Note also that the temporal duration of the plasmoid is somewhat greater than the TCR perturbation observed earlier.

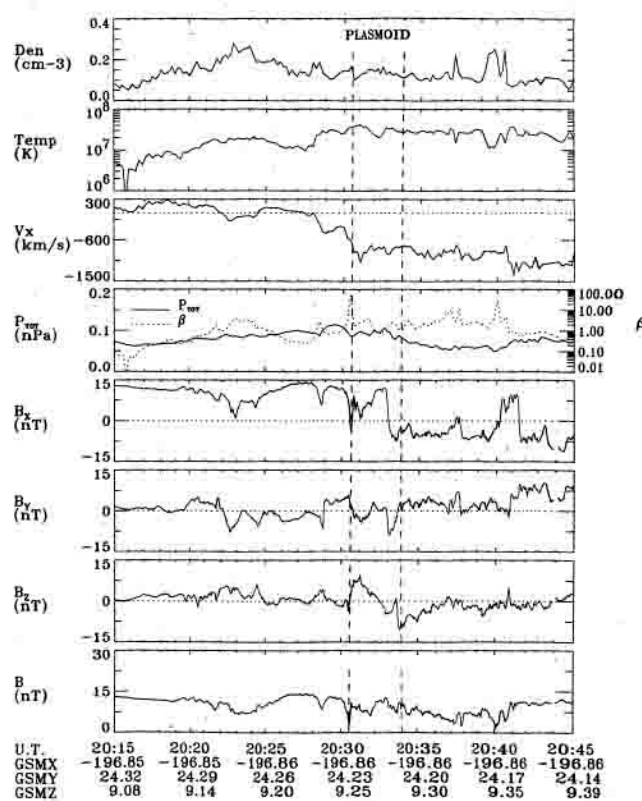


**Figure 2.** Merged plasma and magnetic field measurements (24-s averages) taken by Geotail are displayed for the April 16, 1994, plasmoid event. The low plasma density indicates that the spacecraft was inside of the tail during all of the interval. Note that plasma  $\beta$  varies over 5 orders of magnitude with  $\beta < 1$  generally corresponding to the lobes and the highest values to the plasmoid and postplasmoid plasma sheet.

Given this speed and the  $\sim 3.5$ -min duration of the plasmoid, the estimated length of the plasmoid is  $\sim 22 R_E$ .

The Geotail plasma and magnetic field measurements for the April 16, 1994, plasmoid are displayed in Figure 2. The low ion densities and high temperatures in the top two panels confirm that the spacecraft was indeed inside of the magnetotail during this entire interval. About 2 min before the plasmoid encounter the ion temperature and plasma ion  $\beta$  increase indicating that Geotail was passing first into the outer layers of the plasma sheet or the plasma sheet boundary layer (PSBL) and, later, into the central plasma sheet [e.g., see Zwickl *et al.*, 1984; Slavin *et al.*, 1985]. In fact, the partial reversal in  $B_x$ , the brief, but strong dip in field strength, and the sharp, short increase in  $\beta$  to nearly 100 is due to a brief pass into the high current density center of the cross-tail current layer or so-called "neutral sheet."

The plasmoid, marked with vertical dashed lines, is identified by the north-then-south  $B_z$  variation, the continued southward  $B_z$  afterwards, and the appearance of high-speed tailward flow. As is often the case, the three-dimensional magnetic field variations are quite complex. In this case the spacecraft crossed from the "northern" half of the plasmoid to the "southern" half as indicated by the reversal in  $B_x$  polarity. Note that this current layer is different from the cross-tail current layer observed earlier in that plasma ion  $\beta$ , displayed in the fourth panel, does not change significantly as the layer is crossed. This strongly suggests that this internal "cross-plasmoid" current



**Table 1.** Plasmoid Speeds

Event	$V_{\text{TOP}}$ km/s	$L_{\text{PMD}}$ $R_E$	$\langle V_x \rangle$ km/s	$L_{\text{PMD}}$ $R_E$
April 16, 1994	664	22	827	27
April 17, 1994	405	17	632	27
Sept. 26, 1994	709	40	...	...

layer is a vestige of the cross-tail current layer which has been significantly modified by the magnetic tension forces which will gradually cause the plasmoid to evolve toward a more cylindrical, less stretched magnetic configuration (i.e., plasma ion  $\beta$  is much lower than in the earlier neutral sheet encounter). Given the well defined current layer, it should also be apparent that the magnetic field structure within this plasmoid cannot be well modeled as a quasi-force free flux rope. For example, instead of single maxima in the  $B_x$  and  $B_y$  components typical of such structures [Lepping *et al.*, 1995; Slavin *et al.*, 1995; Khurana *et al.*, 1996] we see instead multiple peaks in  $B_y$  and a bipolar  $B_x$ . Finally, it should also be noted that this event also provides a good example of a relatively unevolved plasmoid which has neither a core of enhanced magnetic field [Slavin *et al.*, 1995] or total magnetic and plasma pressure (A. Ieda *et al.*, submitted manuscript, 1997) which can be used to identify many plasmoids.

The bulk flow speed in the plasmoid and the post-plasmoid plasma sheet is tailward at 700–1000 km/s with a mean value of  $V_x = -827$  km/s. As shown in Table 1, this is significantly greater than the time-of-flight speed of  $-664$  km/s determined earlier and increases the length of the plasmoid to  $27 R_E$ . The  $V_y$  and  $V_z$  components of the flow speed (not shown) were small, i.e., generally  $<100$  km/s, and irregular within the plasmoid. It should also be noted that the flow speed is not highly correlated with the magnetic field direction consistent with the high plasma ion  $\beta$  values of  $\sim 1$ – $30$  observed in the plasmoid and the postplasmoid plasma sheet. In other words, the magnetic field is being carried tailward by this high-speed flow and the distinction between “streaming” and “convection” which can be important in low  $\beta$  regimes is for most purposes moot in this instance.

The energetic particle observations made by the EPIC instrument on Geotail between 2015 and 2045 UT on April 16, 1994, are shown in Plate 1 along with the anisotropies of a number of the particle populations. In the top panel the fluxes of  $\sim 67$  keV ions in the plane of the ecliptic are displayed. The intensity level is color coded as is indicated on the scale to the right of the panel. The vertical axis represents the direction of flow of the ions, such that fluxes of particles traveling sunward (S) appear along a horizontal line through the center of the panel. Conversely, particles traveling tailward (T) appear at the very top or very bottom of the panel. The intensity of particles moving duskward (Du) appear at one fourth of the distance up the plot, while downward (Da) appears at three fourths distance. The next three panels have the same format, but represent the fluxes of 203 keV oxygen ions,  $>38$  keV electrons, and  $9 \text{ keV} < E < 210 \text{ keV}$  protons respectively. The fifth panel represents the fluxes of the latter group of protons as a function of direction out of the ecliptic plane. In this panel, fluxes of particles moving northward appear at the top of the panel, and those moving southward are at the bottom. The center of the panel thus represents the ecliptic plane portion of the distribution of these particles. Note that the

color coded scales for the particle flux is shown on the right for each of the five panels. Also note that the direction of the magnetic field, projected onto the relevant plane is indicated by the dark trace in each panel. In addition, the magnetic field components in GSM coordinates are again presented in the bottom three panels of this figure, while the total field strength is represented by the red line in the first of these panels.

At the start of this interval, the spacecraft is clearly located in the north lobe of the tail, and observes only very low fluxes of energetic particles. Between about 2017 and 2020 UT, a relatively weak beam of ions showing an earthward directed anisotropy can be seen for the energy ranges shown in the first and fourth panels. The 203 keV oxygen ions in the second panel remain at background levels, while the  $>38$  keV electrons exhibit an enhancement of fluxes with a less well defined anisotropy. This period of relatively weak earthward directed fluxes of energetic particles is approximately coincident with the weak earthward flows detected by the low-energy plasma analyzer shown above. Shortly after 2020 UT, there is a sudden increase in the intensity of  $>38$  keV electrons (third panel), now showing a strong tailward streaming distribution. This is followed about a minute later by a similar increase in 67 keV protons (top panel, the  $9 \text{ keV} < E < 210 \text{ keV}$  protons shown in the fourth and fifth panels respond more quickly, but this may be aliased by the longer time resolution for this channel). These data are consistent with the spacecraft crossing a separatrix layer and entering the PSBL. In fact, for the minute or so prior to the sharp increase in the flux of tailward moving 67 keV protons, there is a clear enhancement in the flux of duskward moving particles relative to those moving downward in this channel. This gradient anisotropy is consistent with a region of increased fluxes of these ions moving up over the spacecraft from below, i.e., the correct sense for the PSBL expanding up over a spacecraft located in the northern lobe of the tail [Murphy *et al.*, 1987; Owen and Slavin, 1992]. Also consistent with the picture of Geotail moving into the PSBL or outer plasma sheet shortly after 2020 UT is the slight dip in the magnetic field strength, and its increased variability. The short duration of the electron burst at the edge of this layer may again be consistent with the spacecraft crossing magnetic flux tubes mapping back to the immediate vicinity of an active neutral line. At  $\sim 2030$  UT the bipolar  $B_z$  plasmoid signature begins coincident with a further increase in the flux of 203 keV oxygen ions in the second panel, showing strong tailward streaming. The  $9 \text{ keV} < E < 210 \text{ keV}$  protons shown in the fourth and fifth panels also show a further enhancement, with flow strongly tailward and confined to closely parallel to the ecliptic plane. These energetic ion flows persist until the end of the interval shown, and together with the field and plasma data suggest that the spacecraft remained in a postplasmoid plasma sheet until at least 2050 UT.

In summary, the energetic particle data for the period 2015–2045 UT on April 16, 1994, are consistent with the spacecraft crossing a magnetic separatrix, possibly mapping back to an active reconnection site, shortly after 2020 UT. After residing in the plasma sheet boundary layer for about 10 min, the spacecraft encounters a plasmoid structure, and thereafter remains in the plasma sheet for at least 15 min. The strong tailward nature of the flows after 2020 UT suggest that the particle dynamics are dominated by a reconnection neutral line some way earthward of the spacecraft location. However, for 3–4 min prior to this time, there was a relatively weak earthward beam, suggesting that the spacecraft was on closed field

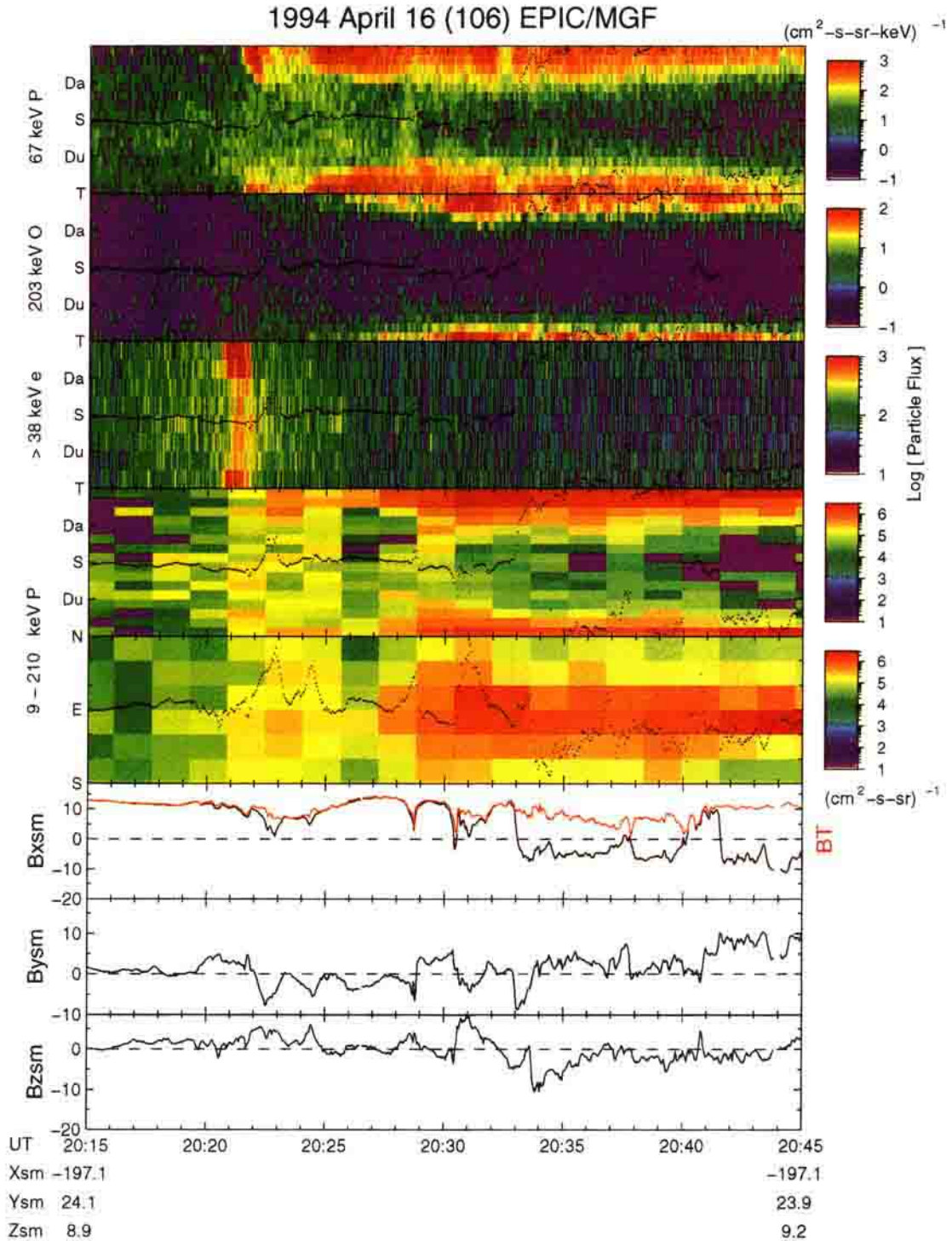


**Plate 1.** Geotail EPIC and MGF observations of energetic particles and magnetic fields for the same interval as Figure 2. A detailed description of the energetic particle fluxes is contained in the text.

lines that mapped to the plasma sheet and neutral line tailward of the spacecraft.

The substorm activity that accompanied the April 16, 1994, event is displayed in Figure 3. To establish the relative timing of the various events, the top panel displays the  $B_z$  component of the magnetic field measured at Geotail with the plasmoid labeled. Similarly, the second panel displays the total magnetic field intensity measured at IMP 8 with the TCR labeled. Pi 2

pulsations were observed at 2003 and 2013 UT at Memambetsu (T. Iyemori, personal communication, 1996). As is customary, the first Pi 2 is taken to indicate the onset of substorm expansion phase which is indicated by a vertical dashed line. Further confirmation of this onset time is found in the Los Alamos National Laboratory energetic electron measurements taken by spacecraft 1984-129 (local time 2034 UT) displayed in the bottom panel. These energetic electrons,  $E \sim 50$  to 300



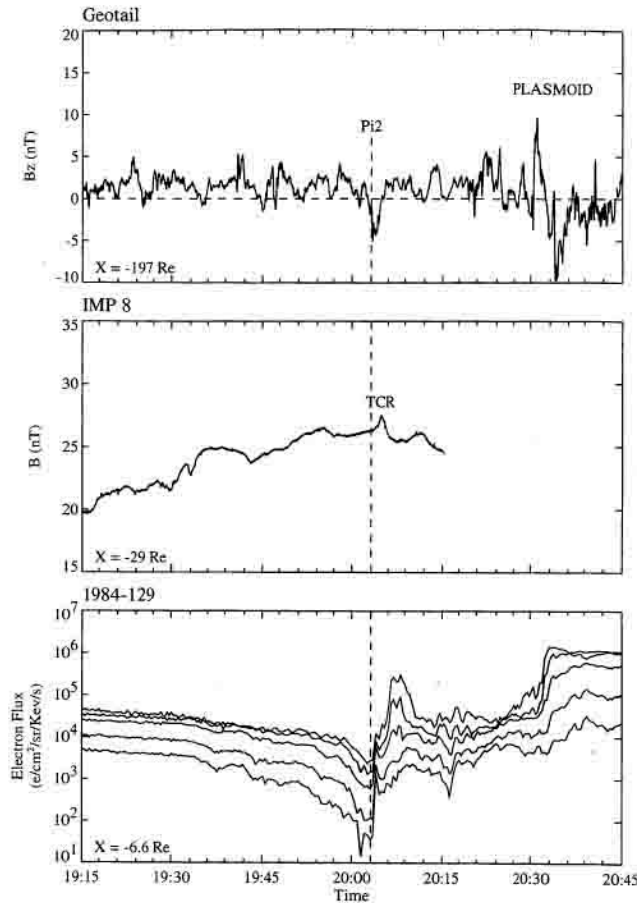


**Figure 3.** Magnetic field measurements showing the time of the TCR at IMP 8 and the plasmoid at Geotail for the April 16, 1994, event are displayed along with spacecraft 1984-129 energetic electron fluxes in five channels. A vertical dashed line marks the time of the first Pi 2 pulsation observed at Memambetsu.

keV, show a nearly dispersionless injection signature within 1 min of the first Pi 2. Against this time line, the TCR at IMP 8 signaling the ejection of the plasmoid down the tail was observed only  $\sim 1$  min after the substorm onset as determined by these two independent means. The decrease in lobe field strength due to open flux reconnection following substorm onset is very clear as remarked upon earlier.

## 2.2. April 17, 1994, Event

The bottom panels of Figure 4 display the IMP 8 magnetic field observations for the April 17, 1994, event. IMP 8 was located at  $X = -30 R_E$ ,  $Y = 12 R_E$ , and  $Z = -4.3 R_E$  and began the interval with the spacecraft emerging from the plasma sheet and entering the south lobe of the tail. Such transitions are usually attributed to plasma sheet thinning as the lobes are loaded with new magnetic flux tubes due to reconnection at the dayside magnetopause [e.g., Fairfield et al., 1981]. The TCR occurs at 0015 UT and is marked with a vertical dashed line. Despite an unfortunate data gap right at the peak of the compression, the usual TCR features are readily apparent. Being observed right at the interface between the plasma sheet and the lobes, such events sample either the outermost layers of the plasmoid proper or the innermost of the lobe flux tubes draped about the plasmoid. Because of the

strong local field intensity, we choose to label this event as a TCR. Following the TCR, the lobe magnetic field exhibits a very broad maximum before beginning to decline after about 0100 UT.

The Geotail magnetic field measurements taken at  $X = -197 R_E$  are displayed in the top panels of Figure 6. As discussed by Kokubun et al. [1996], the first  $\sim 10$  min of this interval found the spacecraft in the magnetosheath. Later, the higher variance, weaker field regions correspond to the plasma sheet and PSBL while the stronger, more steady fields are associated with Geotail being in the tail lobes. The large amplitude north-then-south  $B_z$  perturbation signaling the passage of the plasmoid is centered on  $\sim 0059$  UT and indicated by a pair of vertical dashed lines. As discussed earlier, the field continues to be largely southward for the next  $\sim 20$  min indicating that reconnection between open flux tubes continued to occur earthward of the spacecraft. The time-of-flight speed for the plasmoid between IMP 8 and Geotail is  $167 R_E/44$  min  $\sim 405$  km/s. This speed is only two thirds of that inferred for the previous event, but the longer, 4.5-min duration of this plasmoid produces a very similar length of  $17 R_E$ .

The Geotail magnetic field and plasma measurements for the April 17, 1994, plasmoid are displayed in Figure 5. The very low plasma densities in the top panel show that the spacecraft was in the tail for the entire interval. The north lobe observed

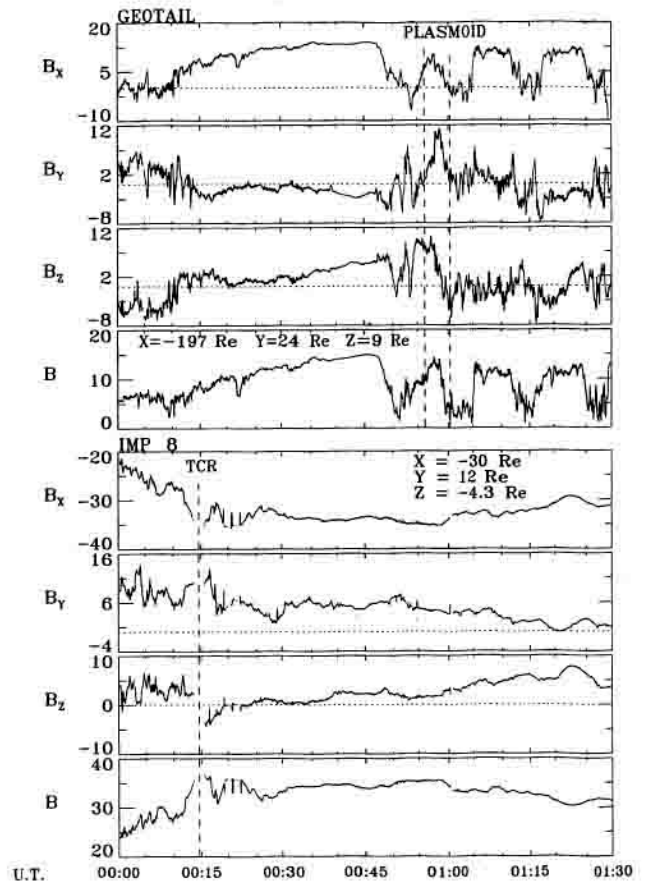


**Figure 4.** Simultaneous 3-s-averaged magnetic field measurements (3-s averages) taken by Geotail and IMP 8 for the interval 0000–0130 UT on April 17, 1994, are displayed in GSM coordinates. For this event the plasmoid at Geotail follows by 44 min the observation of the TCR at IMP 8.

at the beginning of the interval is marked by strong, steady magnetic fields oriented largely along  $X$  as well as low-density and temperature mantle plasma. The plasmoid and postplasmoid plasma sheet are evident in the very high ion temperatures and plasma ion  $\beta$  values of  $\sim 1$  to 300. The PSBL region between the lobe and the initial plasma sheet entry at 0049 UT is indicated by the ion temperatures and plasma ion  $\beta$  values near, but clearly lower than in the plasma sheet and plasmoid proper.

A remarkable aspect of this April 17 event is the bulk flow speed. Just prior to entering the plasma sheet, a  $\sim 2$ -min-long interval of high speed, up to 800 km/s, earthward flow is observed in the PSBL streaming along the field lines up and over the plasmoid. This interpretation is supported by a correlated northward  $V_z$  flow (not shown) with an amplitude of  $\sim 50\%$  of  $V_x$ . When Geotail entered the plasmoid  $\sim 6$  min later, high speed,  $\langle V_x \rangle = -632$  km/s, tailward flow is observed. Within the plasmoid and postplasmoid plasma sheet  $V_y$  and  $V_z$  were generally weak,  $< 100$  km/s. The interval of earthward flow is probably not due to a time variation but rather to the spatial effect of the PSBL being forced upward, past Geotail due to the relatively large  $Z$  dimension of the plasmoid. The existence of this fast earthward flow in the PSBL constitutes strong evidence for ongoing reconnection at a more distant neutral line tailward of Geotail which is populating the PSBL with earthward streaming plasma. Similar earthward flows prior to other Geotail plasmoid encounters have recently been reported by Mukai *et al.* [1996], Hoshino *et al.* [1996], and Kawano *et al.* [1996].

It is also interesting to note that the observed plasmoid and postplasmoid plasma sheet tailward flow speeds were again greater than the speed estimated from the IMP 8 to Geotail flight time for this plasmoid, this time by  $\sim 50\%$  as shown in Table 1. This suggests that for both the April 16 and 17 events, that the plasmoid did not traverse the entire distance from IMP 8 to Geotail at the higher in situ speeds measured at Geotail. Rather, some portion of the flight path must have been traversed at a slower speed either around the time of release or in the more distant tail prior to its encounter with Geotail. In any event, the estimated length of this plasmoid must be revised upward significantly from that based upon the time-of-flight speed to  $632$  km/s  $\times 4.5$  min  $\sim 27 R_E$ .

It is also of interest to examine the magnetic structure of this plasmoid. In contrast with the previous event, this plasmoid does exhibit some aspects of a flux rope-like topology. In Figure 5 there are magnetic field intensity and total thermal and magnetic pressure enhancements within the plasmoid. These features are expected for flux ropes that are becoming force-free and have been used by Slavin *et al.* [1995] and A. Ieda *et al.* (submitted manuscript, 1997) to identify plasmoids with such properties. There are also single maxima in  $B_x$  and  $B_y$  and a broad peak in total field intensity and pressure (e.g., see the force-free flux rope model graphs by Slavin *et al.* [1995]). However, they occur before the transition from positive to southward  $B_z$  and may indicate that the helical fields in this plasmoid are still in process of relaxing toward a force-free configuration [see Hesse *et al.*, 1996a]. In addition, the plasma ion  $\beta$  reaches a minimum just below 1 around the time of peak field strength indicating that magnetic forces were becoming dominate in this core region as required if it is tending toward a force-free magnetic configuration. Similar variations in plasma ion  $\beta$  across plasmoids with strong core magnetic fields have been reported by Frank *et al.* [1994], Machida *et al.* [1994],

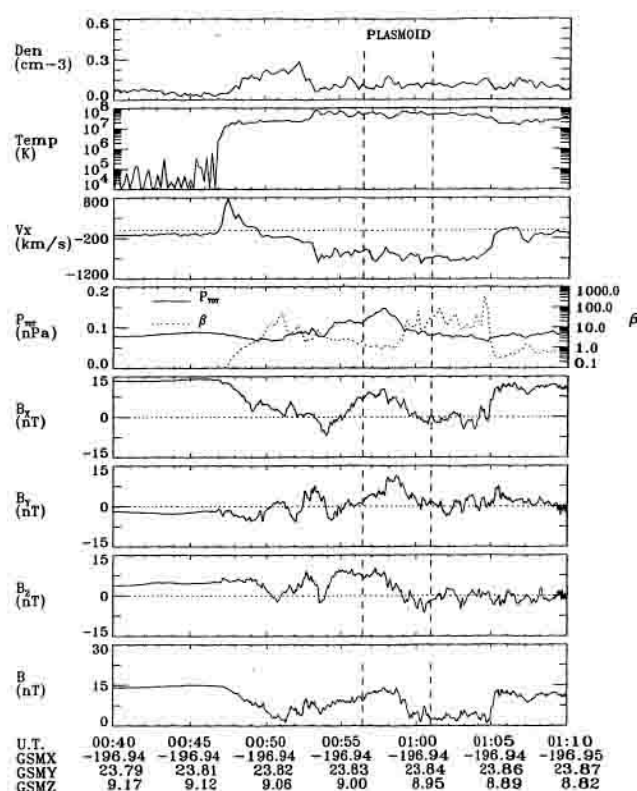


**Figure 5.** Merged plasma and magnetic field measurements taken by Geotail are displayed for the April 17, 1994, plasmoid event. The low plasma density indicates that the spacecraft was inside of the tail during all of the interval. The plasma sheet and plasmoid are generally indicated by ion  $\beta > 1$ .

Mukai *et al.* [1996], and A. Ieda *et al.* (submitted manuscript, 1997).

Another interesting feature of this plasmoid is the unusually large flux of northward  $B_z$  ahead of the plasmoid which may be associated with the plasmoid "snow plowing" into the newly closed positive  $B_z$  magnetic flux tubes being produced at the more distant neutral line. Such an interpretation would be consistent with the fast earthward flows populating the PSBL to the north and south of the plasmoid. Following the plasmoid, Geotail remained in the hot central plasma sheet, plasma ion  $\beta \sim 10$ –300, observing fast tailward flow until 0105 UT when it transitioned back into the PSBL.

The energetic particle observations made by the EPIC instrument between 0040 and 0110 UT on April 17, 1994, are shown in Plate 2, in the same format as Plate 1, described above. From the beginning of the interval shown until 0046 UT, the spacecraft is located in the northern lobe of the magnetotail and observes only very low energetic particle intensities and strong and steady magnetic fields directed predominantly toward the Earth. At 0046 UT, an enhancement of the energetic electron fluxes is detected, although there is not clear directional anisotropy. Shortly thereafter, an increase in earthward directed particles appears in both ion channels (first and fourth panels) and lasts until  $\sim 0050$  UT. Note that these earthward jetting particles are observed contemporaneously with the strong earthward flow of lower-energy plasma described above. In the top panel of Plate 2, there is also some indication of a duskward directed gradient anisotropy, again consistent

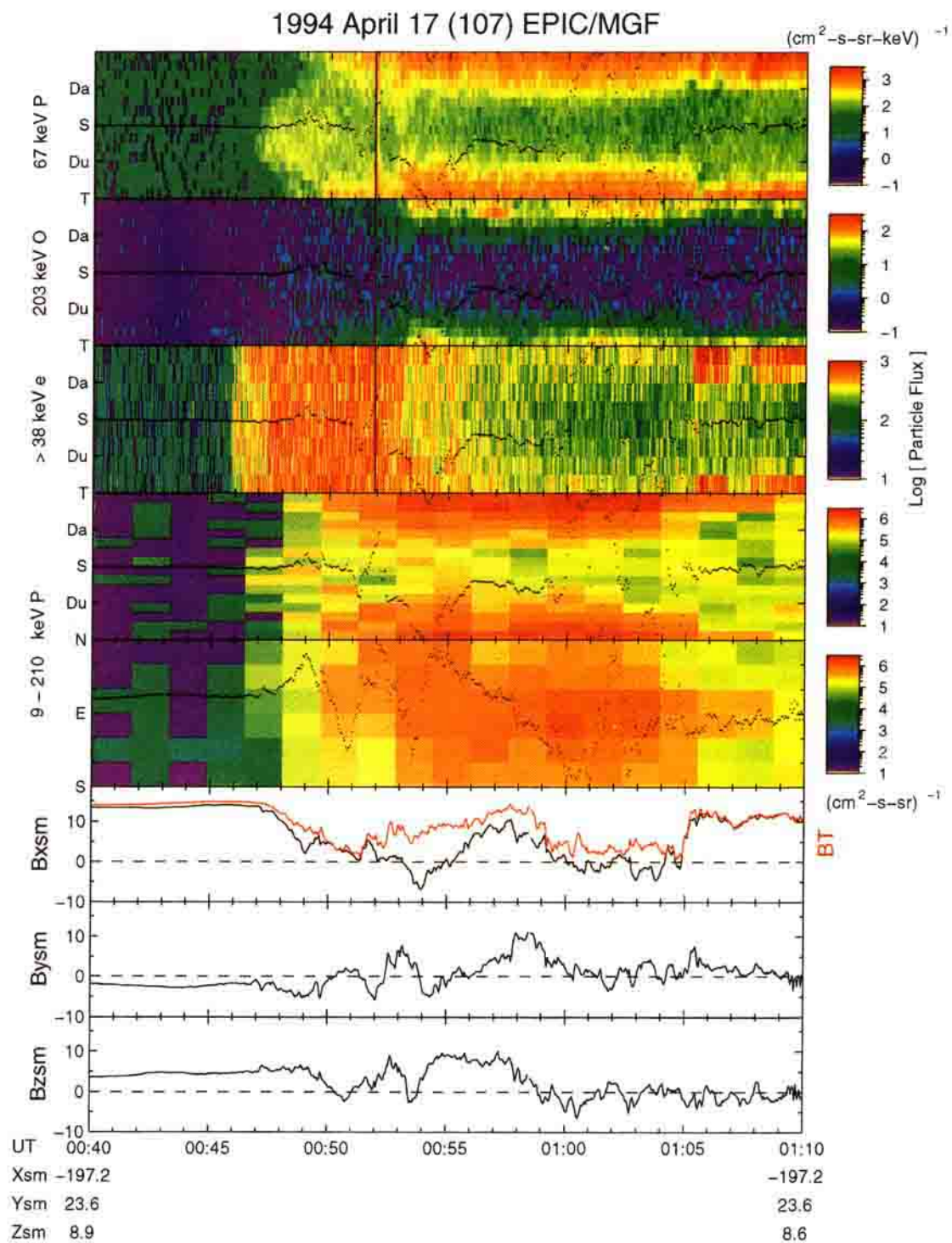


**Plate 2.** Geotail EPIC and MGF observations of energetic particles and magnetic fields for the same interval as Figure 5. A detailed description of the energetic particle fluxes is contained in the text.



with a region of higher concentration energetic particles (i.e., the PSBL) moving northward over a spacecraft located in the northern lobe. Between 0050 and 0053 UT, the sense of the anisotropy in the energetic ion fluxes shown in the first and fourth panel reverses to show tailward streaming distribution. At the same time, the EPIC instrument begins to detect tailward streaming oxygen ions. These features correspond to the interval in which the low-energy plasma instrument detects modest ( $\sim 200$  km/s) tailward plasma flows. At 0053 UT, there is a strong enhancement of fluxes in both the proton channels shown, and in the 203 keV oxygen ions, together with a decline in intensity and a move toward a more tailward directed anisotropy in the  $>38$  keV electrons. This time corresponds to the onset of enhanced tailward flows ( $\sim 6\text{--}700$  km/s) in the lower-energy plasma and is followed about a minute later by the arrival of the plasmoid structure. During the passage of the plasmoid and in the postplasmoid plasma sheet (0102–0105 UT) all the particle populations show strong tailward streaming distributions (panels 1–4), which, at least on the basis of the data shown in the fifth panel, are concentrated closely parallel to the ecliptic plane. At 0105 UT the magnetic field strength recovers almost to its level at the start of the interval shown, and the low-energy plasma flow speeds drops to close to zero. However, the magnetic field data retains some variability, suggesting that the spacecraft has remained in the PSBL, rather than returned to the lobe proper. This suggestion is confirmed by the continued presence of tailward streaming energetic ion populations and also intense fluxes of tailward streaming  $>38$  keV electrons. Hence the spacecraft may again be located on flux tubes that map back to the neutral sheet in the vicinity of an active neutral line. This neutral line must be located earthward of the spacecraft location.

In summary, the energetic particle data for the period 0040–0110 UT on April 17, 1994, are consistent with the spacecraft crossing a magnetic separatrix, possibly mapping back to an active reconnection site, at 0046 UT. For  $\sim 3\text{--}4$  min, the spacecraft observes earthward directed anisotropies in the proton channels and omnidirectional, but elevated, intensities of  $>38$  keV electrons. These data suggest that at this time the particle dynamics in this region are controlled by an active reconnection site tailward of the spacecraft location. After 0050 UT, there is a strong enhancement of 203 keV oxygen fluxes, and all the particle populations shown in Plate 2 show a strong tailward anisotropy, consistent with the classical picture of a plasmoid passage past the spacecraft.

The substorm conditions associated with this plasmoid event are displayed in Figure 6. The top and middle panels show the Geotail  $B_z$  and IMP 8 total field values with the plasmoid and TCR events marked. A series of Pi 2 pulsations were observed on the ground at Wingst and Memambetsu between 0009 and 0118 UT (T. Iyemori, personal communication, 1996). A vertical dashed line is shown to indicate the time of the first Pi 2 which we take to indicate substorm expansion phase onset. This was followed  $\sim 3$  min later by an energetic electron injection at 1990-095, which was located at  $\sim 2300$  LT. The TCR at IMP 8 indicates that plasmoid release took place  $\sim 6$  and 3 min later than the first Pi 2 and the injection at 1990-095, respectively. Hence, as with the April 16 event, plasmoid ejection appears to occur within a few minutes of substorm expansion phase.

### 2.3. September 26, 1994, Event

The bottom panels of Figure 7 display the IMP 8 magnetic field measurements for the interval 0500–0630 UT on Septem-

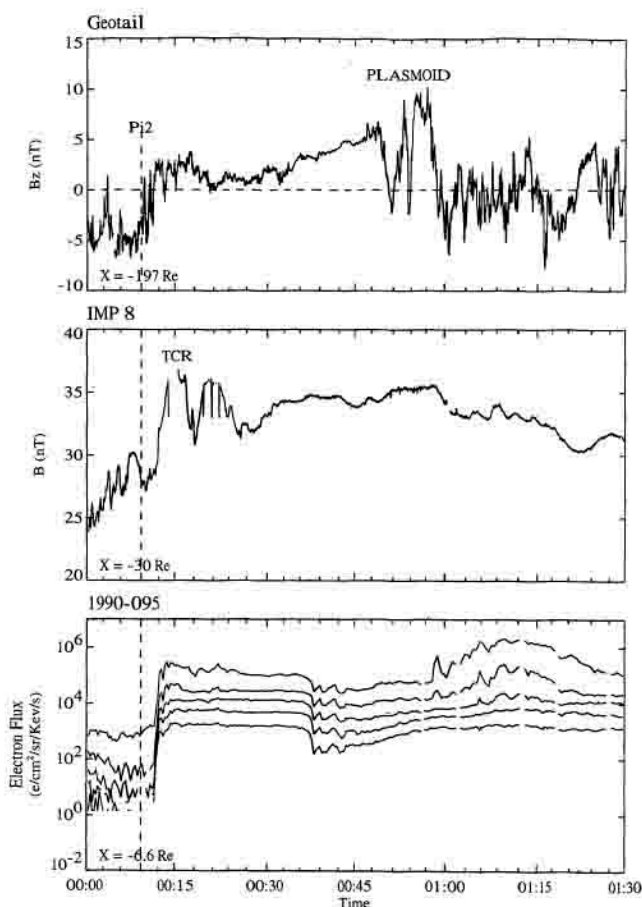


**Figure 6.** Magnetic field measurements showing the time of the TCR at IMP 8 and the plasmoid at Geotail for the April 17, 1994, event are displayed along with spacecraft 1990-095 (2254 LT) energetic electron fluxes in five channels. A vertical dashed line marks the time of the first Pi 2 pulsation observed at Memambetsu.

ber 26, 1994. The steady magnetic fields oriented largely in the  $X$  direction indicate that IMP 8 was in the north lobe for the entire interval. The TCR is observed at 0533 UT after the lobe magnetic field had increased by 15% over the preceding half hour. The effects of tail flaring considered in detail by Taguchi *et al.* [1997] are very pronounced for this event with  $B_z$  being negative prior to the TCR and then going positive afterward as open lobe flux tubes are closed by reconnection and the tail relaxes into a lower energy, less flared state. In order for reconnection between the open field lines in the tail to occur and “unload” the lobes, closed field line reconnection must first eject a plasmoid so the open flux tubes in the lobes come together at the near-Earth  $X$  line and rapidly merge [Hesse *et al.*, 1996b].

The Geotail magnetic field observations in the top panels show that this spacecraft was also mostly in the north lobe at  $X = -170 R_E$  prior to the large north-then-south  $B_z$  variation centered on 0553 UT. As with the previous cases the  $B_z$  component for the magnetic field was southward for  $\sim 20$  min following the plasmoid as would be expected if reconnection continued to take place at a neutral line earthward of Geotail. However, the relatively strong magnetic fields observed throughout the event suggest that Geotail never penetrated deeply into the plasmoid or plasma sheet during this event.

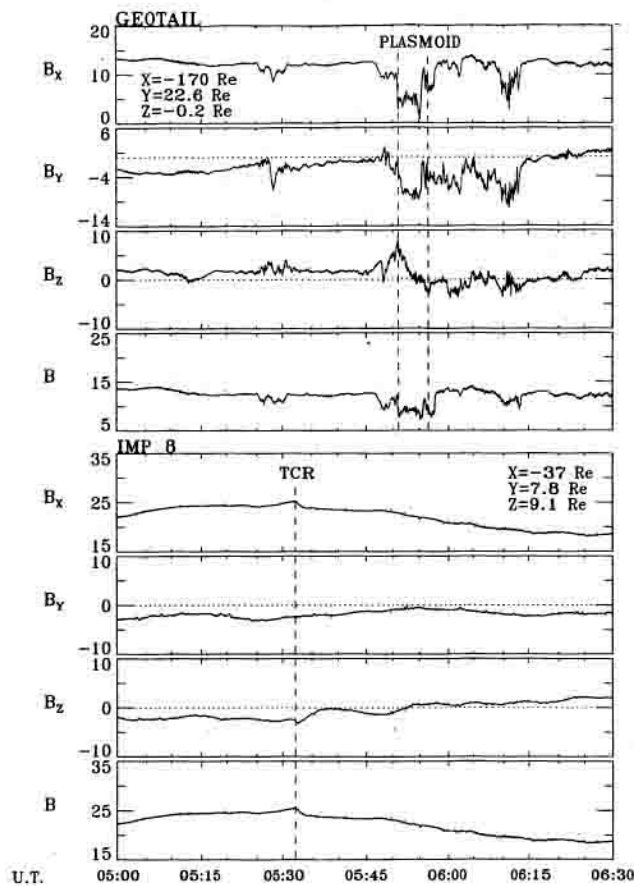


**Figure 7.** Simultaneous averaged magnetic field measurements (3-s averages) taken by Geotail and IMP 8 for the interval 0500–0630 UT on September 26, 1994, are displayed in GSM coordinates. For this event the plasmoid at Geotail follows by 18 min the observation of the TCR at IMP 8.

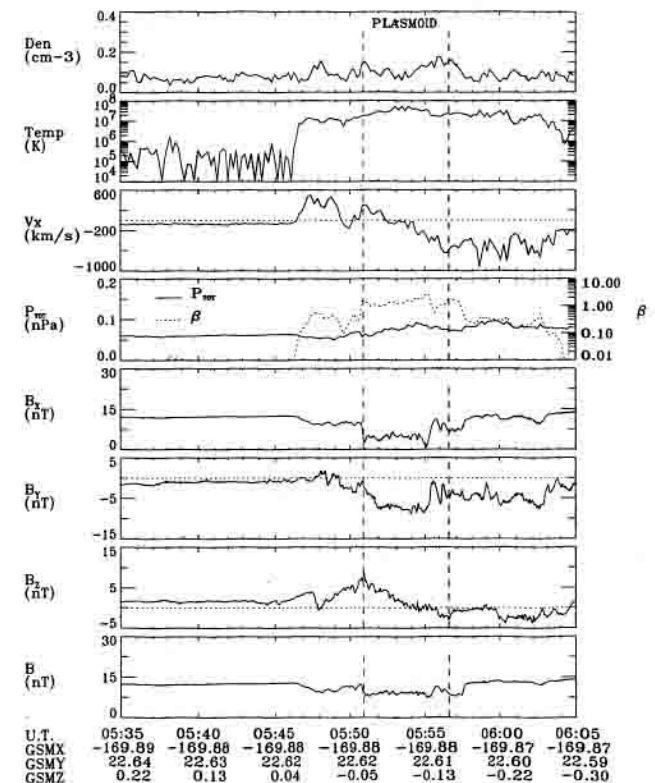
The time-of-flight speed from IMP 8 to Geotail is  $133 R_E / 20 \text{ min} \sim 709 \text{ km/s}$ . On the basis of the 6-min duration of the plasmoid, its estimated length is  $\sim 40 R_E$ .

Figure 8 displays the Geotail plasma and magnetic field measurements for the September 26 plasmoid event. The low ion density across the entire interval indicates that the spacecraft was always in the magnetotail. In fact, there is very little density variation anywhere except for a small enhancement within the "plasmoid." Just as with the previous event, the interval begins with Geotail in the north lobe of the tail as inferred from the low mantle ion temperatures and extremely low lobe plasma ion  $\beta$  values. About 4 min prior to the plasmoid the PSBL is entered as the oncoming plasmoid pushes the PSBL over the spacecraft. The PSBL is identified by the greatly enhanced ion temperatures, the weakened magnetic field intensity and the intermediate plasma ion  $\beta$  values of 0.1–1. As with the preceding April 17, 1994, event, fast earthward flow is observed in the PSBL suggesting, again, the presence of an active reconnection site tailward of Geotail.

This event is different, however, in that Geotail appears to just graze the plasmoid as reflected by the fact that plasma ion  $\beta$  only slightly exceeds unity at any point within the plasmoid. Such events have been termed by *Moldwin and Hughes [1992c]* as "boundary layer plasmoids." This interpretation is supported by the plasma flow velocity which does not become

tailward until the middle of this plasmoid event. In the higher-resolution LEP energy-time spectrograms (not shown), the hot earthward plasma flows gradual decrease in intensity during this interval as tailward ion beams become dominant producing the low net bulk flow speeds. It is not until the plasmoid has passed Geotail that the flow reaches a relatively steady tailward value of 600 km/s. In this case, the magnetic fields are strong in the sense of  $\beta \leq 1$  and the observed flow may be regarded as "streaming" along the magnetic field. Such flows cannot be properly used to estimate plasmoid dimensions or to make comparisons with the time-of-flight speed from IMP 8 to Geotail. This interpretation is supported by the northward  $V_z$  flow (not shown) during the first portion of the encounter where  $V_x$  was earthward. Accordingly, no entry has been made in Table 1 for the in situ plasma speed for this event. Finally, as with the April 17 event, where there was also evidence for a near-by distant neutral line in the form of high-speed earthward flow, there is an over abundance of positive  $B_z$  relative to the negative  $B_z$  in this plasmoid.

The energetic particle observations made by the EPIC instrument between 0535 and 0605 UT on April 26, 1994, are shown in Plate 3, in the same format as Plate 1, described above. These observations show many of the same features seen in the previous two cases. At the start of the interval, the spacecraft is located in the north lobe and observes very low energetic particle fluxes. At 0546 UT, there is a short (<1 min)



**Figure 8.** Merged plasma and magnetic field measurements taken by Geotail are displayed for the September 26, 1994, plasmoid event. The low plasma density indicates that the spacecraft was inside of the tail during all of the interval. However, the low plasma ion  $\beta \sim 1$  in the plasmoid and lower elsewhere indicates that only the other layers of the plasmoid and the PSBL were encountered, not the core region of the plasmoid or the plasma sheet proper.

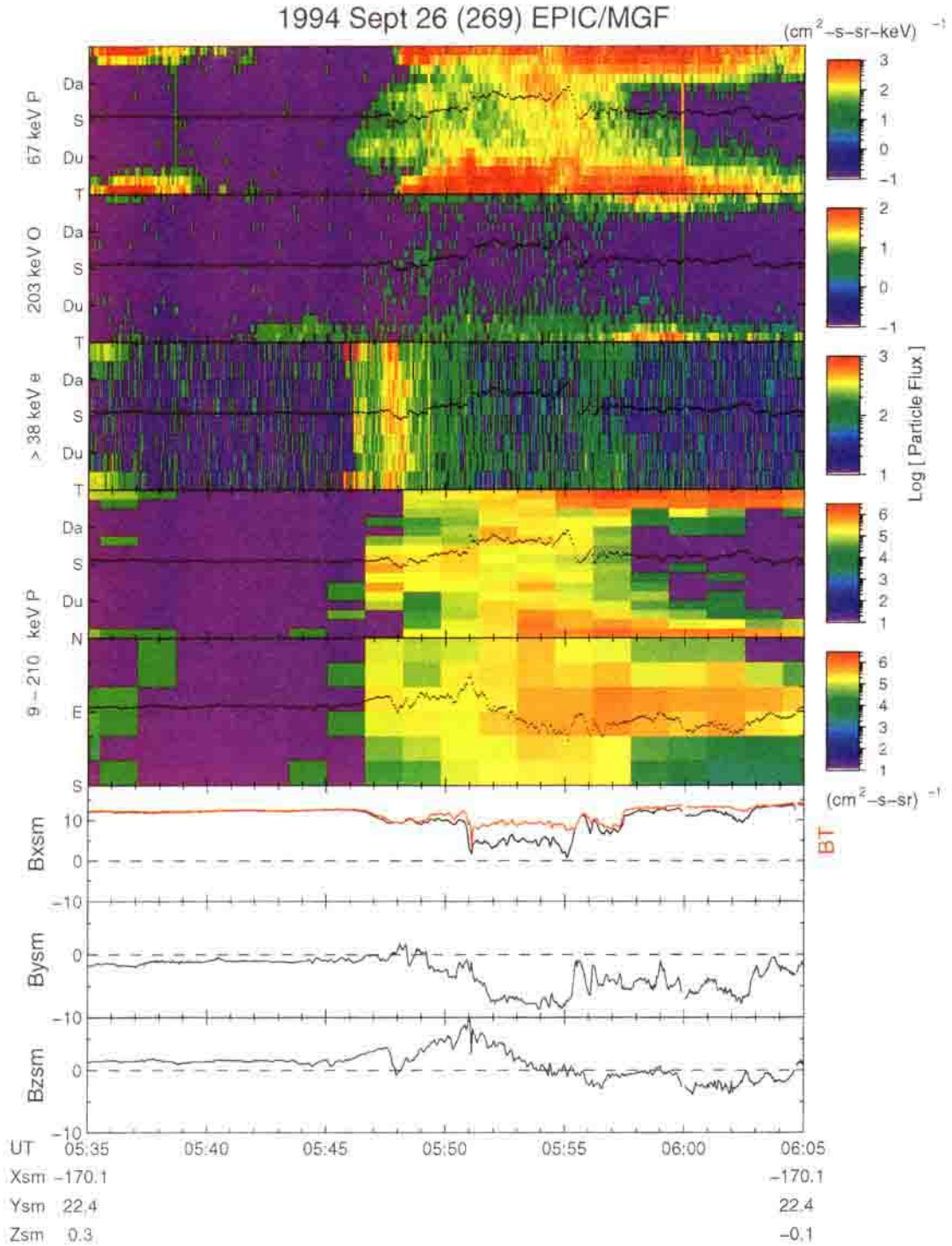


**Plate 3.** Geotail EPIC and MGF observations of energetic particles and magnetic fields for the same interval as Figure 8. A detailed description of the energetic particle fluxes is contained in the text.

burst of tailward propagating energetic electrons followed immediately by a less intense bidirectional (earthward/tailward) beam of these particles (third panel). At the same time the magnetic field strength shows the slight depression characteristic of an entry into the PSBL, and the clear duskward anisotropy shown by the  $\sim 67$  keV ions in the top panel between 0546 and 0548 UT is consistent with this region moving up over the spacecraft location from below. At 0547 UT, there is another short burst of  $>38$  keV electrons, which shows no clear direc-

tional anisotropy. Also, between  $\sim 0547$  and  $\sim 0550$  UT,  $9 \text{ keV} < E < 210 \text{ keV}$  protons in the fourth panel show a clear earthward anisotropy, although the  $\sim 67$  keV protons in the upper panel show strong tailward streaming in the later part of this interval. Since the former population is probably dominated by particles in the lower part of the energy range, it seems that the lower-energy particles are moving earthward at this time, while the higher-energy particles are predominately moving tailwards. Consistent with this interpretation, the low-



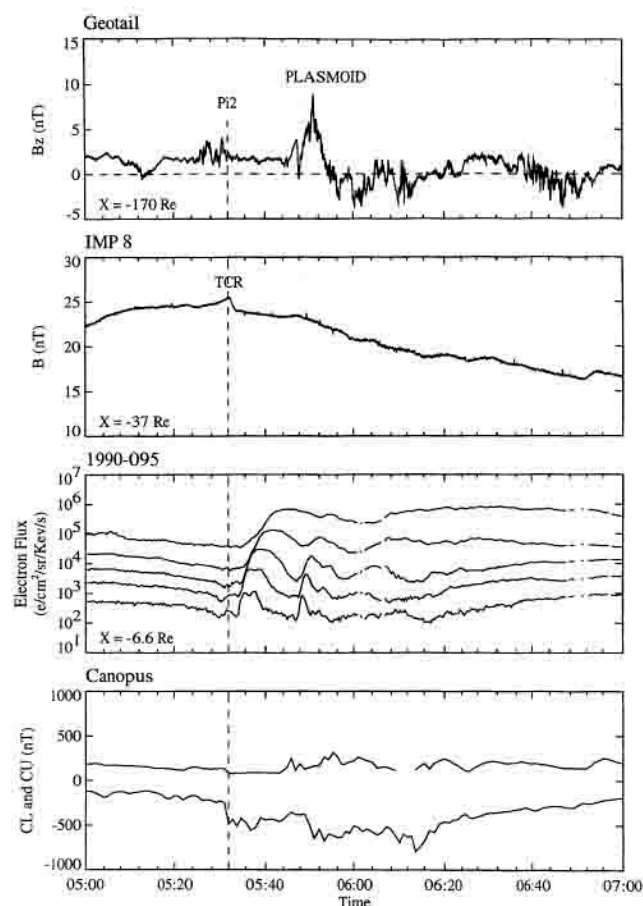


**Figure 9.** Magnetic field measurements showing the time of the TCR at IMP 8 and the plasmoid at Geotail for the September 26, 1994, event are displayed in the top panels. Energetic electron fluxes in five channels from spacecraft 1990-095 (0416 LT) and the CANOPUS CU and CL indices are in the bottom panels. A vertical dashed line marks the time of the first Pi 2 pulsation observed at Memambetsu.

energy plasma instrument data shown above indicate earthward plasma flows of around 400 km/s during this period. However, during the plasmoid passage itself (~0550 to ~0557 UT) and the postplasmoid plasma sheet (~0557 to ~0603 UT), both proton channels show predominantly tailward streaming distributions, consistent with the classical plasmoid picture.

In summary, the energetic particles are consistent with the spacecraft crossing a magnetic separatrix at ~0546 UT, as evidenced by the appearance of an enhanced beam of electrons. The tailward direction of this beam suggests that this separatrix maps back to an active reconnection site earthward of the spacecraft location. However, the data suggest that between this burst and the arrival of the plasmoid, the lower-energy particle dynamics, which show earthward flows, are dominated by the effects of a neutral line tailward of the spacecraft location while higher energy particles show tailward anisotropies. This implies that the spacecraft may be located on closed loop flux tubes that have been reconnected at both the near-Earth and distant tail neutral lines but that reconnection at the near-Earth occurred later, or at a greater distance from the spacecraft than in the distant tail, such that only the faster tailward streaming particles have had time to reach the

spacecraft location. Hence, although substorm onset will be shown to have occurred at ~0532 UT, the dynamic effects of a distant neutral line (i.e., the earthward flow observed prior to the plasmoid arrival at Geotail) can again be observed in the deep tail for some time after substorm onset, and disconnection of the plasmoid.

The substorm conditions associated with this plasmoid event are displayed in Figure 9. The top and middle panels show the Geotail  $B_z$  and IMP 8 total field values with the plasmoid and TCR events marked. Pi 2 pulsations were observed on the ground at Memambetsu at 0532 and 0546 UT (T. Iyemori, personal communication, 1996). A vertical dashed line is shown to indicate the time of the first Pi 2 and hence substorm expansion phase onset. This result is confirmed by the negative bay in the CANOPUS CL index which serves as a proxy for  $AL$  in this local time sector. About 2 min later a dispersive energetic electron injection is observed at S/C 1990-095 which located at approximately 0416 LT. The TCR at IMP 8 indicates that plasmoid release took place within a minute of the first Pi 2 and before the dispersive injection drifted to spacecraft 1990-095. Hence, as with the two previous events, plasmoid ejection appears to occur very near substorm expansion phase onset.

### 3. Discussion

The well-known obstacles to obtaining multipoint observations of dynamic events within the magnetosphere have been well borne out by this study. During the interval examined IMP 8 crossed the magnetotail 33 times with a typical traversal lasting ~2.2 days (N.B., the IMP 8 orbital period is 12.2 days). Given the ~50% tracking coverage of IMP 8 during this era, the total duration of the tail observations collected by IMP 8 during the study interval was ~36 days. Assuming ~3–4 substorms per day [Borovsky *et al.*, 1993], perhaps 100–150 substorms should have occurred while IMP 8 was in the tail and returning measurements. The 10 events identified would correspond to ~7–10% of the substorms having produced TCR at IMP 8, which is just slightly less than the frequencies of occurrence reported by Slavin *et al.* [1990] and Taguchi *et al.* [1997]. Of these 10 events, Geotail was then found to have been in the tail for just three of the events at IMP 8 (see Figures 1, 3, 6, and 9).

The finding of plasmoids in the Geotail measurements for all three of the IMP 8 events for which Geotail was in the magnetotail provides important support for plasmoids as a readily reproducible substorm phenomenon. Furthermore, the ISTP era substorm observations provided by geosynchronous spacecraft- and ground-based magnetometer stations have allowed us to clearly demonstrate the role of plasmoid ejection in the magnetic flux transfer cycle implicit in the NENL model [McPherron *et al.*, 1973]. The lobe is first loaded with additional flux tubes by dayside reconnection, the plasma sheet separating the two flux laden lobes is then pinched off and ejected tailward in the form of a plasmoid, and, within a few minutes, the substorm expansion phase proceeds powered by the dissipation of stored magnetic energy from the lobes.

A primary objective of this study was the comparison of direct measurement of how fast plasmoids move down the tail in contrast with the time-of-flight method which has been applied previously to the ISEE 3 and Geotail plasmoid/TCR populations [Baker *et al.*, 1987; Slavin *et al.*, 1993; Nagai *et al.*, 1994]. In our study, TOF speeds were determined using the observation of the center of TCR at IMP 8 as the start and the

arrival time of the midpoint of the plasmoid at Geotail as the start time. As summarized in Table 1, TOF downtail speeds of  $\sim 400$ – $700$  km/s, respectively, were determined for these plasmoid events in excellent agreement with the range of values reported in earlier studies [Richardson *et al.*, 1987; Ieda *et al.*, 1997]. Comparison with the in situ plasma bulk speeds for the first two plasmoids, where Geotail penetrated deeply into the plasmoid, show the in situ speeds to be higher than the TOF speeds by 25 and 56%, respectively. These speed differences are much greater than the nominal  $\sim 10\%$  accuracy of LEP bulk flow speeds in the plasma sheet. Such a discrepancy could be readily explained by the existence of a finite acceleration time following the release of the plasmoid. In fact, such gradual acceleration of plasmoids with increasing downtail distance have been reported previously [Gloeckler *et al.*, 1984; Ieda *et al.*, 1997]. However, a unique determination of how the plasmoid forms, evolves with time, and moves downtail using a small number of two-spacecraft events is of course not possible, but these results may stimulate further theoretical modeling and statistical analysis.

A two spacecraft study of plasmoid ejection similar to this one was conducted by Moldwin and Hughes [1992b] using the IMP 8 and ISEE 3 measurements. Despite large data gaps due to a lack of onboard tape recorders, one clear example of a TCR at IMP 8 followed by a plasmoid at ISEE 3 ( $X = -168 R_E$ ) was found. Interestingly, there was an unusually long time delay between the two spacecraft compared with the events in this study of  $\sim 71$  min. However, the extremely slow time-of-flight speed indicated by these observations,  $\sim 200$  km/s, was confirmed by the ISEE 3 bulk speed measurements taken within the plasmoid. By comparison, the 20- to 44-min transit times between IMP 8 and Geotail at  $X = -170$  to  $-197 R_E$  found in this study are in excellent agreement with the mean 30-min delays for transit to  $X \sim -200 R_E$  determined by superposed epoch and regression analyses of plasmoid and TCR arrival times [Nagai *et al.*, 1994; Slavin *et al.*, 1993; Baker *et al.*, 1987].

A second objective of this study is the comparison of the plasmoid lengths determined by Geotail to the downstream distance of IMP 8 at the time of its TCR observations. It is at once apparent that with lengths of  $\sim 27$  to  $40 R_E$  (see Table 1) these plasmoids could not have formed completely earthward of IMP 8 given its location at  $X = -29$  to  $-37 R_E$ . Rather, as argued by Slavin *et al.* [1990] and Taguchi *et al.* [1997], the IMP 8 TCR draping signatures must be associated only with the Earthward portion of plasmoids forming, for the most part, farther down the tail. Such an interpretation, as pointed out by this earlier studies, is consistent with the relative weakness of the leading northward  $B_z$  perturbation relative to the trailing southward  $B_z$  portion of the typical IMP 8 TCR signature.

While not the primary objective of this study, the events considered here have offered an opportunity to examine the structure of plasmoids in the distant tail. It is well known that plasmoids do not generally exhibit a minimum in field intensity at their center as would be expected if they resembled the O-type neutral lines depicted in some simple cartoons. Rather, the field strength is relatively constant or a strong "core" field may be present near the inflection point in the north-then-south  $B_z$  variation [Slavin *et al.*, 1989]. Moldwin and Hughes [1992a] and Ieda *et al.* [1997] surveyed a large number of plasmoids in the ISEE 3 deep-tail data set and found that the magnetic signatures associated with many plasmoids were consistent with helical field topologies. In addition, Lepping *et al.*

[1995, 1996], Slavin *et al.* [1995], and Khurana *et al.* [1995] have demonstrated that the magnetic fields within some plasmoids observed by Geotail, ISEE 3, and Galileo could be well fitted using force-free flux rope models. These modeling studies also indicated that central axes of plasmoids with flux rope topologies are generally along the GSM Y direction. While plasmoids made up of perfectly closed loops with no connection to the outside environment, as sometimes portrayed in cartoons, are not possible in the reality of three-dimensions, it is not known what fraction of plasmoids eventually evolve to have force-free flux rope cores. It is interesting to note that of the two cases in this study where Geotail penetrated deeply into plasmoids one exhibited magnetic field variations which were consistent with a quasi-flux rope topology and one did not. This result supports the recent studies which suggest that plasmoids have a complex, highly variable magnetic structure [e.g., Mukai *et al.*, 1996]. Although this study was largely concerned with plasmoid kinematics, these events clearly demonstrate the need for multipoint observations of the internal evolution of the plasmoid with increasing downtail distance.

The nature of the energetic particle flows in the outer portions of plasmoids have also been investigated in this study. Previously, Owen and Slavin [1992] examined the anisotropies within energetic ( $E > 15$  keV) ion enhancements associated with traveling compression regions observed by ISEE 3. In about half of all TCRs encountered earthward of  $X = -100 R_E$ , the observed anisotropies indicated that the ion dynamics were at least partially controlled by the effects of a more distant neutral line. Hence distant neutral lines may be active during plasmoid ejection and result in plasmoids continuing to encounter newly closed magnetic flux tubes as they move tailward. This view is strongly supported by the energetic particle measurements reported in this study where separatrix layers and earthward/tailward streaming could be clearly be seen before/after the plasmoid encounters. Hoshino *et al.* [1996] and Kawano *et al.* [1996] report that earthward thermal plasma flows are often observed just prior to plasmoid passage and its associated fast tailward flows. More specifically, they observe an earthward beam of plasma in the outer PSBL and bidirectional [Hoshino *et al.*, 1996] or tailward [Kawano *et al.*, 1996] streaming in the inner PSBL. Again, this would mean that the tailward moving plasmoid may still be surrounded by flux tubes recently closed at a distant neutral line. Such a scenario was originally suggested by Nishida *et al.* [1986] on the basis of his study of slowly moving, "quasi-stationary" plasmoids with ISEE 3 observations. Further evidence of active reconnection sites tailward of Geotail during plasmoid encounters was presented by Mukai *et al.* [1996] in his study of plasma distribution functions within plasmoids and the surrounding PSBL. Despite the dominance of strong tailward bulk flows, they reported earthward jetting components in many of the individual distributions continues until the ejection of a new plasmoid forces it out the far end of the tail.

Given the scenario for plasmoid formation and ejection just described, some scale length estimates can be made as follows. The time  $\tau_A$  for a signal to propagate from the earthward edge of the plasmoid bulge, where the open flux tubes are draped around it, to the distant X line can be roughly estimated as  $\tau_A = \Delta X/V_A$ . Here  $\Delta X$  is the distance between the earthward edge of the plasmoid bulge and the distant X line and  $V_A$  is the Alfvén speed in the recently reconnected lobe flux tubes,  $\sim 10^3$  km/s based upon averages over the cis-lunar tail lobes [Slavin *et al.*, 1985, 1994]. When  $\tau_A$  is larger than the characteristic

time for closing the open flux tubes at the distant X line,  $\tau_{SR}$ , the magnetic field and plasma dynamics at the distant X line are largely unaffected by the near-Earth reconnection and tailward motion of the plasmoid bulge. At this stage the whole region between NENL and the distant X line probably should not be considered as a plasmoid in the sense of it being a single cohesive structure because different parts of this region between the two X lines can move independently with different bulk flow velocities. The distance  $\Delta X$  will decrease with time as the plasmoid bulge moves toward the distant X line. It is reasonable to assume that the distant X line "learns" that a new NENL has formed when  $\tau_A$  become comparable with  $\tau_{SR}$ . At this stage the dynamic consequences of the reconnection in the vicinity of the distant X line can be observed, e.g., in the expansion of the PSBL in the  $\pm Z$  directions. A knowledge of the reconnection rate at the distant X line should in principle allow us to estimate plasmoid dimensions,  $\Delta X$ , as this region begins to behave as a cohesive structure, i.e., when  $\tau_A \sim \tau_{SR}$ . For example, let us assume that the characteristic time for closing the open flux tubes at the distant X line,  $\tau_{SR}$ , is about 3 min. This time is consistent with a simple estimate  $\tau_{SR} \sim L_z/V_z$ , where  $L_z$  is a characteristic thickness for the distant current sheet, e.g.,  $\sim 1 R_E$ , and  $V_z$  is a characteristic convection speed into the reconnection region, e.g.,  $\sim 35$  km/s. For  $\tau_{SR} \sim 3$  min and  $V_A \sim 10^3$  km/s, the condition  $\tau_A \sim \Delta X/V_A \sim \tau_{SR}$  yields a plasmoid length of  $\Delta X \sim V_A \tau_{SR} \sim 28 R_E$ . This value is in reasonable agreement with average plasmoid lengths derived in this study and the 10–60  $R_E$  values found by earlier statistical studies [Richardson et al., 1987; Moldwin and Hughes, 1992a; Slavin et al., 1993; Nagai et al., 1994; A. Ieda et al., submitted manuscript, 1997].

#### 4. Summary

In summary, these ISTP multispacecraft observations have shown that (1) the events presented here, and the one studied earlier by Moldwin and Hughes [1992b], confirm that TCRs at IMP 8 are indeed associated with the ejection of plasmoids down the tail; (2) the plasmoid lengths measured by Geotail,  $\sim 27$  to  $40 R_E$ , require that at least a portion of plasmoid formation take place beyond the IMP 8 orbit; (3) for the two events in which Geotail passed deeply into the plasmoid, the measured bulk speeds were significantly larger than the time-of-flight speeds between IMP 8 and Geotail suggesting some additional acceleration after their initial release; (4) all three of our events exhibited tail lobe flux loading/unloading and/or growth phase plasma sheet thinning (depending upon the spacecraft trajectory through the regions of the tail); (5) in each case plasmoid release took place at or within a few minutes of substorm expansion phase onset; and (6) the energetic particle and magnetic field observations suggest that reconnection at a preexisting active distant X line near  $X = -200 R_E$  continues to add magnetic flux to the plasmoid and populate the surrounding PSBL with earthward streaming plasma as it is ejected tailward.

Finally, we have discussed the implications of these results for plasmoid formation/ejection and presented analytic arguments which predict plasmoid length scales comparable to those reported here and elsewhere. These results are important because a thorough and, ultimately, quantitative understanding of where and why reconnection takes place in the tail and how these neutral lines move and evolve during substorms is essential to future progress in the understanding of magne-

total dynamics. In addition, other important processes may play critical roles in preparing the magnetosphere for reconnection to take place and they, too, must be understood [e.g., Lui et al., 1991]. It is hoped that the further analysis and distillation of ISTP events such as those presented here will build the foundation for major advances in theory and modeling.

**Acknowledgments.** The contribution of Pi 2 observations by T. Iyemori (Kyoto University) and CANOPUS magnetic indices (P. I.-G. Rostoker) are gratefully acknowledged. The assistance of E. Mazur with computational aspects of this research are also acknowledged.

The Editor thanks W. Jeffrey Hughes and L. A. Frank for their assistance in evaluating this paper.

#### References

- Baker, D. N., R. C. Anderson, R. D. Zwickl, and J. A. Slavin, Average plasma and magnetic field variations in the distant magnetotail associated with near-Earth substorm effects, *J. Geophys. Res.*, **92**, 71, 1987.
- Behlke, A., E. T. Sarris, G. Tsiropoulou, R. W. McEntire, S. Kokubun, and T. Yamamoto, Energetic particle bursts detected by Geotail in the distant tail, *Proceedings of Third International Conference on Substorms*, edited by S. Perraut, A. Roux, and J. Suavaud, *Eur. Space Agency Spec. Publ.*, ESA SP-389, 487–492, 1996.
- Birn, J., M. Hesse, and K. Schindler, Filamentary structure of a three-dimensional plasmoid, *J. Geophys. Res.*, **94**, 241, 1989.
- Borovsky, J. E., R. J. Nemzek, and R. D. Belian, The occurrence rate of magnetospheric substorm onsets: Random and periodic substorms, *J. Geophys. Res.*, **98**, 3897, 1993.
- Caan, M. N., R. L. McPherron, and C. T. Russell, Substorm and interplanetary magnetic field effects on the geomagnetic tail lobes, *J. Geophys. Res.*, **80**, 191, 1975.
- Fairfield, D. H., R. P. Lepping, E. W. Hones Jr., S. J. Bame, and J. R. Asbridge, Simultaneous measurements of magnetotail dynamics by IMP spacecraft, *J. Geophys. Res.*, **86**, 1396, 1981.
- Frank, L. A., W. R. Paterson, K. L. Ackerson, S. Kokubun, T. Yamamoto, D. H. Fairfield, and R. P. Lepping, Observations of plasmas associated with the magnetic signature of a plasmoid in the distant magnetotail, *Geophys. Res. Lett.*, **21**, 2967, 1994.
- Gloeckler, G., M. Scholer, F. M. Ipavich, D. Hovestadt, A. B. Gavin, and B. Klecker, Characteristics of suprathermal  $H^+$ ,  $He^{++}$  in plasmoids in the distant magnetotail, *Geophys. Res. Lett.*, **11**, 1030, 1984.
- Hesse, M., and J. Birn, Plasmoid evolution in an extended magnetotail, *J. Geophys. Res.*, **91**, 5683, 1991.
- Hesse, M., J. Birn, M. M. Kuznetsova, and J. Dreher, A simple model of core field generation during plasmoid evolution, *J. Geophys. Res.*, **101**, 10,797, 1996a.
- Hesse, M., J. Birn, D. N. Baker, and J. A. Slavin, MHD simulations of the transition of magnetic reconnection from closed to open field lines, *J. Geophys. Res.*, **101**, 10,805, 1996b.
- Hones, E. W., Jr., The magnetotail: Its generation and dissipation, in *Physics of Solar Planetary Environments*, edited by D. J. Williams, pp. 559–571, AGU, Washington, D. C., 1976.
- Hones, E. W., Jr., Substorm processes in the magnetotail: Comments on "On hot tenuous plasmas, fireballs, and boundary layers in the Earth's magnetotail" by L. A. Frank et al., *J. Geophys. Res.*, **82**, 5633, 1977.
- Hones, E. W., Jr., D. N. Baker, S. J. Bame, W. C. Feldman, J. T. Gosling, D. J. McComas, R. D. Zwickl, J. A. Slavin, E. J. Smith, and B. T. Tsurutani, Structure of the magnetotail at  $200 R_E$  and its response to geomagnetic activity, *Geophys. Res. Lett.*, **11**, 5, 1984.
- Hoshino, M., T. Mukai, A. Nishida, Y. Saito, T. Yamamoto, and S. Kokubun, Evidence of two active reconnection sites in the distant magnetotail, *J. Geomagn. Geoelectr.*, **48**, 515, 1996.
- Kawano, H., et al., A flux rope followed by recurring encounters with traveling compression regions: Geotail observations, *Geophys. Res. Lett.*, **21**, 2891, 1994.
- Kawano, H., et al., A quasi-stagnant plasmoid observed with Geotail on October 15, 1993, *J. Geomagn. Geoelectr.*, **48**, 525, 1996.
- Kennel, C. F., The Kiruna conjecture: The strong version, in *Proceed-*



- ings of First International Conference on Substorms, *Eur. Space Agency Spec. Publ., ESA SP-335*, 509–601, 1992.
- Khurana, K. K., M. G. Kivelson, L. A. Frank, and W. R. Paterson, Observations of magnetic flux ropes and associated currents in the Earth's magnetotail with the Galileo spacecraft, *Geophys. Res. Lett.*, 22, 2087, 1995.
- Kivelson, M. G., K. K. Khurana, R. J. Walker, L. Kepko, and D. Xu, Flux ropes, interhemispheric conjugacy and magnetospheric current closure, *J. Geophys. Res.*, 101, 27,341, 1996.
- Kokubun, S., T. Yamamoto, M. H. Acuna, K. Hayashi, K. Shiokawa, and H. Kawano, The Geotail magnetic field experiment, *J. Geomagn. Geoelectr.*, 46, 7, 1994.
- Kokubun, S., L. A. Frank, K. Hayashi, Y. Kamide, R. P. Lepping, T. Mukai, R. Nakamura, W. R. Paterson, T. Yamamoto, and K. Yumoto, Large field events in the distant magnetotail during magnetic storms, *J. Geomagn. Geoelectr.*, 48, 561, 1996.
- Lepping, R. P., D. H. Fairfield, J. Jones, L. A. Frank, W. R. Paterson, S. Kokubun, and T. Yamamoto, Cross-tail magnetic flux ropes as observed by the Geotail spacecraft, *Geophys. Res. Lett.*, 22, 1193, 1995.
- Lepping, R. P., J. A. Slavin, M. Hesse, J. A. Jones, and A. Szabo, Analysis of Magnetotail Flux Ropes with Strong Core Fields: ISEE 3 Observations, *J. Geomagn. Geoelectr.*, 48, 589, 1996.
- Lui, A. T. Y., C. L. Chang, A. Mankofsky, H. K. Wong, and D. Winske, A cross-field current instability for substorm expansions, *Geophys. Res.*, 96, 11,389, 1991.
- Machida, S., T. Mukai, Y. Saito, T. Obara, T. Yamamoto, and S. Kokubun, Geotail low energy particle and magnetic field observations of a plasmoid at  $X = 142 R_E$ , *Geophys. Res. Lett.*, 21, 2295, 1994.
- McPherron, R. L., C. T. Russell, and M. P. Aubry, Satellite studies of magnetospheric substorms on August 15, 1968, 9, Phenomenological model for substorms, *J. Geophys. Res.*, 78, 3131, 1973.
- Moldwin, M. B., and W. J. Hughes, Plasmoids as flux ropes, *J. Geophys. Res.*, 96, 14,051, 1991.
- Moldwin, M. B., and W. J. Hughes, On the formation and evolution of plasmoids: A survey of ISEE 3 data, *J. Geophys. Res.*, 97, 19,259, 1992a.
- Moldwin, M. B., and W. J. Hughes, Multi-satellite observations of plasmoids: IMP 8 and ISEE 3, *Geophys. Res. Lett.*, 19, 1081, 1992b.
- Moldwin, M. B., and W. J. Hughes, Plasmoid observations in the distant plasma sheet boundary layer, *Geophys. Res. Lett.*, 19, 1911, 1992c.
- Moldwin, M. B., and W. J. Hughes, Geomagnetic substorm association of plasmoids, *J. Geophys. Res.*, 98, 81, 1993.
- Mukai, T., S. Machida, Y. Saito, M. Hirahara, T. Terasawa, N. Kaya, T. Obara, M. Ejiri, and A. Nishida, Low Energy Particle (LEP) experiment onboard the Geotail satellite, *J. Geomagn. Geoelectr.*, 46, 669, 1994.
- Mukai, T., M. Fujimoto, M. Hoshino, S. Kokubun, S. Machida, K. Maezawa, A. Nishida, Y. Saito, T. Terasawa, and T. Yamamoto, Structure and kinetic properties of plasmoids and their boundary regions, *J. Geomagn. Geoelectr.*, 48, 541, 1996.
- Murphy, N., J. A. Slavin, D. N. Baker, and W. J. Hughes, Enhancement of energetic ions associated with traveling compression regions in the deep geomagnetic tail, *J. Geophys. Res.*, 92, 64, 1987.
- Nagai, T., K. Takahashi, H. Kawano, T. Yamamoto, S. Kokubun, and A. Nishida, Initial Geotail survey of magnetic substorm signatures in the magnetotail, *Geophys. Res. Lett.*, 21, 2991, 1994.
- Nishida, A., M. Scholer, T. Terasawa, S. J. Bame, G. Gloeckler, E. J. Smith, and R. D. Zwickl, Quasi-stagnant plasmoid in the middle tail: A new pre-expansion phase phenomenon, *J. Geophys. Res.*, 91, 4245, 1986.
- Ogino, T., R. J. Walker, and M. Ashour-Abdalla, Magnetic flux ropes in 3-D MHD simulations, *Physics of Magnetic Flux Ropes*, *Geophys. Monogr. Ser.*, vol. 58, edited by C. T. Russell et al., AGU, Washington, D. C., 1990.
- Owen, C. J., and J. A. Slavin, Energetic ion events associated with traveling compression regions, *Proceedings of International Conference on Substorms*, *Eur. Space Agency Spec. Publ., ESA SP-335*, 365–370, 1992.
- Raeder, J., Global MHD simulation of the dynamics of the magnetosphere: Weak and strong solar wind forcing, in *Substorms 2, Proceedings of Second International Conference on Substorms*, edited by J. R. An, J. D. Craven, and S.-I. Akasofu, pp. 561–568, Univ. of Alaska, Fairbanks, 1994.
- Richardson, I. G., et al., Plasmoid-associated energetic ion bursts in the deep geomagnetic tail: Properties of plasmoids and the post-plasmoid plasma sheet, *J. Geophys. Res.*, 92, 9997, 1987.
- Schindler, K., A theory of the substorm mechanism, *J. Geophys. Res.*, 79, 2803, 1974.
- Scholer, M., G. Gloeckler, D. Hovestadt, B. Klecker, and F. M. Ipavich, Characters of plasmoid-like structures in the distant magnetotail, *J. Geophys. Res.*, 89, 8872, 1984.
- Slavin, J. A., E. J. Smith, B. T. Tsurutani, D. G. Sibeck, H. J. Singer, D. N. Baker, J. T. Gosling, E. W. Hones, and F. L. Scarf, Substorm-associated traveling compression regions in the distant tail: ISEE 3 observations, *Geophys. Res. Lett.*, 11, 657, 1984.
- Slavin, J. A., E. J. Smith, D. G. Sibeck, D. N. Baker, R. D. Zwickl, and S.-I. Akasofu, An ISEE 3 study of average and substorm conditions in the distant magnetotail, *J. Geophys. Res.*, 90, 10,875, 1985.
- Slavin, J. A., et al., CDAW 8 observations of plasmoid signatures in the geomagnetic tail: An assessment, *J. Geophys. Res.*, 94, 15,153, 1989.
- Slavin, J. A., R. P. Lepping, and D. N. Baker, IMP 8 observations of traveling compression regions: New evidence for near-Earth plasmoids and neutral lines, *Geophys. Res. Lett.*, 17, 913, 1990.
- Slavin, J. A., M. F. Smith, E. L. Mazur, D. N. Baker, T. Iyemori, H. J. Singer, and E. W. Greenstadt, ISEE 3 plasmoid and TCR observations during an extended interval of substorm activity, *Geophys. Res. Lett.*, 19, 825, 1992.
- Slavin, J. A., M. F. Smith, E. L. Mazur, D. N. Baker, T. Iyemori, and E. W. Greenstadt, ISEE 3 observations of traveling compression regions in the Earth's magnetotail, *J. Geophys. Res.*, 98, 15,425, 1993.
- Slavin, J. A., C. J. Owen, and M. Hesse, The evolution of the plasmoid-lobe interaction with downtail distance, *Geophys. Res. Lett.*, 21, 2765, 1994.
- Slavin, J. A., C. J. Owen, M. M. Kuznetsova, and M. Hesse, ISEE 3 observations of plasmoids with flux rope magnetic topologies, *Geophys. Res. Lett.*, 22, 2061, 1995.
- Taguchi, S., J. A. Slavin, and R. P. Lepping, IMP 8 observations of traveling compression regions in the mid-tail near substorm expansion phase onset, *Geophys. Res. Lett.*, 24, 353, 1997.
- Walker, R. J., and T. Ogino, A global MHD simulation of the origin and evolution of magnetic flux ropes in the magnetotail, *J. Geomagn. Geoelectr.*, 48, 765, 1996.
- Williams, D. J., R. W. McEntire, C. Schlemm II, A. T. Y. Lui, G. Gloeckler, S. P. Christon, and F. Gliem, GEOTAIL Energetic Particles and Ion Composition Instrument, *J. Geomagn. Geoelectr.*, 46, 39, 1994.
- Zong, Q.-G., B. Wilken, I. A. Daglis, S. Livi, J. Woch, G. D. Reeves, T. Doke, T. Iyemori, T. Mukai, T. Yamamoto, S. Kokubun, Z.-Y. Pu, and S. Ullaland, Geotail observations of energetic ion species and magnetic fields in plasmoid-like structures in the course of a substorm, in *Proceedings of Third International Conference on Substorms*, *Eur. Space Agency Spec. Publ., ESA SP-389*, 619–624, 1996.
- Zwickl, R. D., et al., Evolution of the Earth's distant magnetotail: ISEE 3 electron plasma results, *J. Geophys. Res.*, 89, 11,007, 1984.
- D. H. Fairfield, M. M. Kuznetsova, R. P. Lepping, and J. A. Slavin, Laboratory for Extraterrestrial Physics, NASA Goddard Space Flight Center, Greenbelt, MD 20771.
- S. Kokubun, Solar-Terrestrial Environment Laboratory, Nagoya University, Toyokawa, Aichi 464-01, Japan.
- A. T. Y. Lui, Applied Physics Laboratory, Johns Hopkins University, Laurel, MD 20723.
- T. Mukai, Y. Saito, and T. Yamamoto, Institute of Space and Astronautical Science, 3-1-1 Yoshinodai, Sagami-hara, Kanagawa 229, Japan.
- C. J. Owen, Queen Mary and Westfield College, Astronomy Unit, London, England, United Kingdom.
- G. D. Reeves, Los Alamos National Laboratory, Los Alamos, NM 87545.
- S. Taguchi, Department of Electronic Engineering, University of Electro-Communications, Tokyo, Japan.

(Received January 15, 1997; revised May 14, 1997; accepted July 24, 1997.)